



## Prediction of shear strength of corrosion reinforced concrete beams using Artificial Neural Network

Panagiotis G. Asteris<sup>1</sup>, Thuy-Anh Nguyen<sup>2\*</sup>

<sup>1</sup>Computational Mechanics Laboratory, School of Pedagogical and Technological Education, Heraklion, GR 14121, Athens, Greece

<sup>2</sup>University of Transport Technology, Hanoi 100000, Vietnam

### Article info

#### Type of article:

Original research paper

#### DOI:

<https://doi.org/10.58845/jstt.utt.2022.en.2.2.1-12>

#### \*Corresponding author:

E-mail address:

[anhnt@utt.edu.vn](mailto:anhnt@utt.edu.vn)

**Received:** 07/12/2021

**Revised:** 29/04/2022

**Accepted:** 02/05/2022

**Abstract:** The shear strength of corroded reinforced concrete (CRC) beams is a critical consideration during the design stages of RC structures. In this study, we propose a machine learning technique for estimating the shear strength of CRC beams across a range of service periods. To do this, we gathered 158 CRC beam shear tests and used Artificial Neural Network (ANN) to create a forecast model for the considered output. Twelve input variables indicate the geometrical and material properties, reinforcing parameters, and the degree of corrosion in the beam, whereas the shear strength is the output considered. The database is designed to employ 70 percent of the data point to train the model and 30 percent to assess the performance. The model makes outstanding predictions, according to the results, with an  $R^2$  value of 0.989. In addition, five empirical shear strength models in the literature are utilized to test the suggested ANN model, demonstrating that the new model performs much better. With any given service period, the suggested time-dependent prediction model can offer the shear strength of CRC beams.

**Keywords:** Artificial Neural Network, Corrosion Reinforced concrete beams, Shear strength.

### 1. Introduction

In reinforced concrete (RC) constructions, corrosion of reinforcing bars is one of the most prevalent causes of early deterioration, which results in reduced service life. The corrosion of reinforcing bars has been demonstrated to impair the load capacity of RC members in previous studies [1]–[4]. Corrosion also reduces the area of reinforcement, has an effect on the mechanical characteristics of reinforcing bars [5], and causes a loss of bonding qualities between the steel reinforcement and the concrete matrix [4], [6]. This means that failure modes may shift from flexural to shear even if the beams are well-designed in the first place. As a result, it is vital to precisely forecast

the shear strength of corroded RC (CRC) beams, especially during their entire life cycle, in order to ensure the structural integrity and safety of the structures [7].

A number of analytical or empirical formulas for determining CRC beams' shear strength have been developed to date, including those based on the strut-and-tie model (STM) [8], [9], modified compression field theory [9], equivalent truss theory [10], limit equilibrium theory [11], and design codes (i.e., ACI 318-02, ACI 318-08, ACI 318-14) [8], [9], [12]. In Lu et al. recently [13], a detailed assessment of a large number of empirical shear strength models for CRC beams was completed. This resulted in developing a unique model for

predicting the shear strength of concrete reinforced concrete (CRC) beams, which exceeded all prior empirical models. These models also include corrosion effects by reducing or modifying the parameters of the models, and they have shown strong agreement with a number of experimental data, notably those of their own. However, there are several more studies that have been done and published in the literature [8], [9], [14], raise questions regarding whether they can produce appropriate predictions or not. Furthermore, there are few comparative studies between these models, and the models involved, when corrosion damage variables are taken into account, are pretty limited.

Some research on the application of numerical modeling approaches has also been done [15]–[17]. These techniques, however, are static and cannot be applied to datasets that are not the same as the ones for which they were created. Natural phenomena involved in corrosion include nonlinear features, which most people fail to consider. Because corrosion is a natural process, its characteristics are likely to be non-linearly linked to the corrosion property under investigation. As a result, linear relationships are insufficient to represent the process. Models must be recalibrated with fresh data sets to become more general. It will take a significant amount of time and work to regenerate fresh sets of coefficients in order to develop a new model in this manner.

A novel strategy that uses machine learning (ML) techniques to build a prediction model using existing data has lately gained widespread interest throughout the globe. Problems related to structural engineering [18], [19], materials science [20]–[22], geotechnical [23], [24] have been successfully solved. It should be noted that some relevant research has been undertaken utilizing machine learning to predict the shear strength of RC components, which has been shown to be effective [25]–[27]. To the authors' knowledge, research in estimating the shear strength of CRC beams is limited. In the most current work by Fu

and Feng [7], a machine learning model based on the gradient boosting regression tree (GBRT) algorithm was constructed to estimate the shear strength of corroded reinforced concrete beams. The performance of the model is shown through statistical criteria with  $R^2 = 0.955$ , RMSE = 19.19 kN and MAE = 12.84 kN. This study proposes a machine learning model that predicts the shear strength of CRC beams to improve the prediction performance.

Machine learning algorithms such as Artificial Neural Network (ANN) are considered powerful tools for solving nonlinear, complex, and exceptional cases in which the relationship between inputs and outputs cannot be easily established explicitly. The capacity of the ANN model to self-learn and alter the weights, for example, allows the calculation results to be compatible with reality without the need for mechanical, physical, and chemical equations as well as subjective judgment to be taken into consideration. Consequently, the fundamental goal of this research is to investigate and apply the ANN model to the prediction of the shear strength of CRC beams.

## 2. Database construction

A data set encompassing 158 instances related to the shear strength of CRC beam obtained from 11 references [4], [10], [11], [28]–[34], was used to develop the prediction model. Single-layer tension-reinforced beams are used in [10], [30], [33], whereas double-layer tension-reinforced beams are used in [32]. Tension and compression reinforcements are used to strengthen the remaining beams. Rectangular beams make up all of the specimens. Electrochemical accelerated corrosion experiments without loading were used to cause corrosion in all of the specimens.

A total of 12 input variables can be found in the database, namely compressive strength of concrete ( $X_1$ ), beam section width ( $X_2$ ) and section depth ( $X_3$ ), longitudinal reinforcement ratio ( $X_4$ ) and stirrup ratio ( $X_5$ ), yield strength of longitudinal reinforcement ( $X_6$ ), yield strength of stirrup ( $X_7$ ),

stirrup spacing ( $X_8$ ), ratio of shear span-to-depth ( $X_9$ ), a section loss ratio of longitudinal reinforcement ( $X_{10}$ ), a section loss ratio of the

stirrup ( $X_{11}$ ), section effective depth ( $X_{12}$ ), and the considered output variable is the ultimate shear strength ( $Y$ ).

**Table 1.** The input and output parameters used in the development of ANN model.

Parameter	Mean	Std	Min	Median	Max
Compressive strength of concrete ( $X_1$ - MPa)	28.118	7.110	20.000	27.140	44.400
Beam section width ( $X_2$ - mm)	159.190	37.534	120.000	150.000	254.000
Depth ( $X_3$ - mm)	257.342	98.488	180.000	230000	610.000
Longitudinal reinforcement ratio ( $X_4$ - %)	2.1662	0.462	1.220	2.150	3.270
Stirrup ratio ( $X_5$ - %)	0.360	0.187	0.140	0.320	0.900
Yield strength of longitudinal reinforcement ( $X_6$ - MPa)	430.595	109.767	210.000	416.000	706.000
Yield strength of stirrup ( $X_7$ - MPa)	397.462	109.628	275.000	335.000	626.000
Stirrup spacing ( $X_8$ - mm)	155.677	47.590	80.000	150.000	305.000
Ratio of shear span-to-depth ( $X_9$ )	2.326	0.896	1.000	2.000	4.700
Section loss ratio of longitudinal reinforcement ( $X_{10}$ )	3.017	5.126	0.000	0.000	26.000
Section loss ratio of the stirrup ( $X_{11}$ )	23.436	23.968	0.000	20.876	97.200
Section effective depth ( $X_{12}$ - mm)	215.018	90.952	130.000	184.000	521.000
Ultimate shear strength ( $Y$ - kN)	119.546	94.146	26.600	99.000	594.000

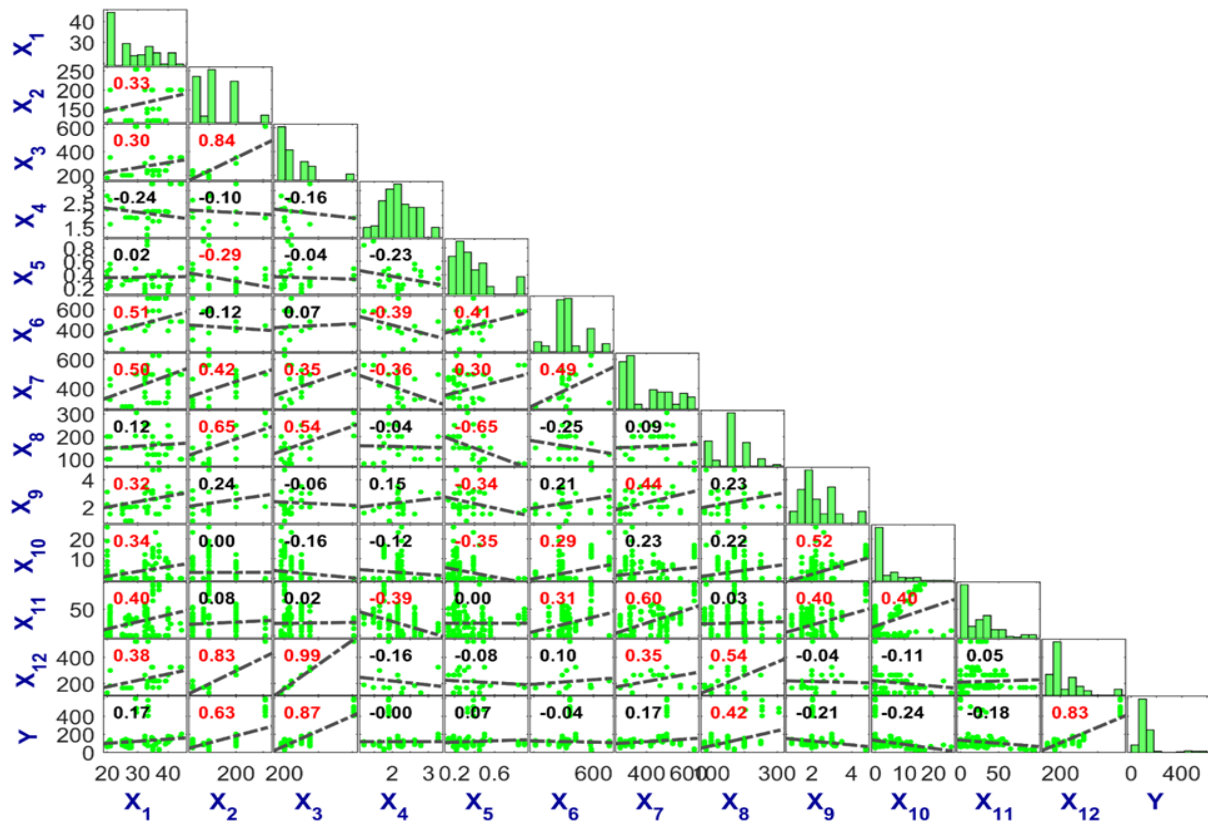


**Fig. 1.** The distribution chart and correlation between input and output parameters are considered in this study

Because all specimens are simply supported beams, the shear span is computed from the concentrated load center to the support center for all specimens, regardless of their design. Table 1 contains statistical information on the input and output variables utilized in this study, including mean values, minimum and maximum values, standard deviation (StD), and median.

The distribution graphs of the input and output parameters and the correlation between them are shown in Fig. 1. Each pair of parameters had its Pearson correlation coefficient computed and reported. To reduce mistakes that may occur during ANN simulation, the values of the input and output parameters are normalized to be between 0 and 1. This technique is frequently used in artificial intelligence challenges to reduce the number of mistakes caused by numerical simulations.

**3. Model Details**

**3.1. Artificial Neural Network**

Artificial Neural Network (ANN) is based on how the human brain functions. It stimulates the biological nervous system, consisting of many layers of neurons (nodes) linked together via connections. A weight is applied to each node. An artificial neural network (ANN) is a "computational system" that receives inputs and generates outputs (Baughman 1995).

The ANN processes are mathematically expressed and generalized as:

$$y_i = f\left(\sum_j w_{ij}x_j + \mu_i\right) \tag{1}$$

where  $x_j$  are the neuron's inputs,  $w_{ij}$  is the weight vector associated with those inputs,  $\mu_i$  is the threshold, offset, or bias, where  $f()$  represents the transfer function, and  $y_i$  represents the neuron's output.

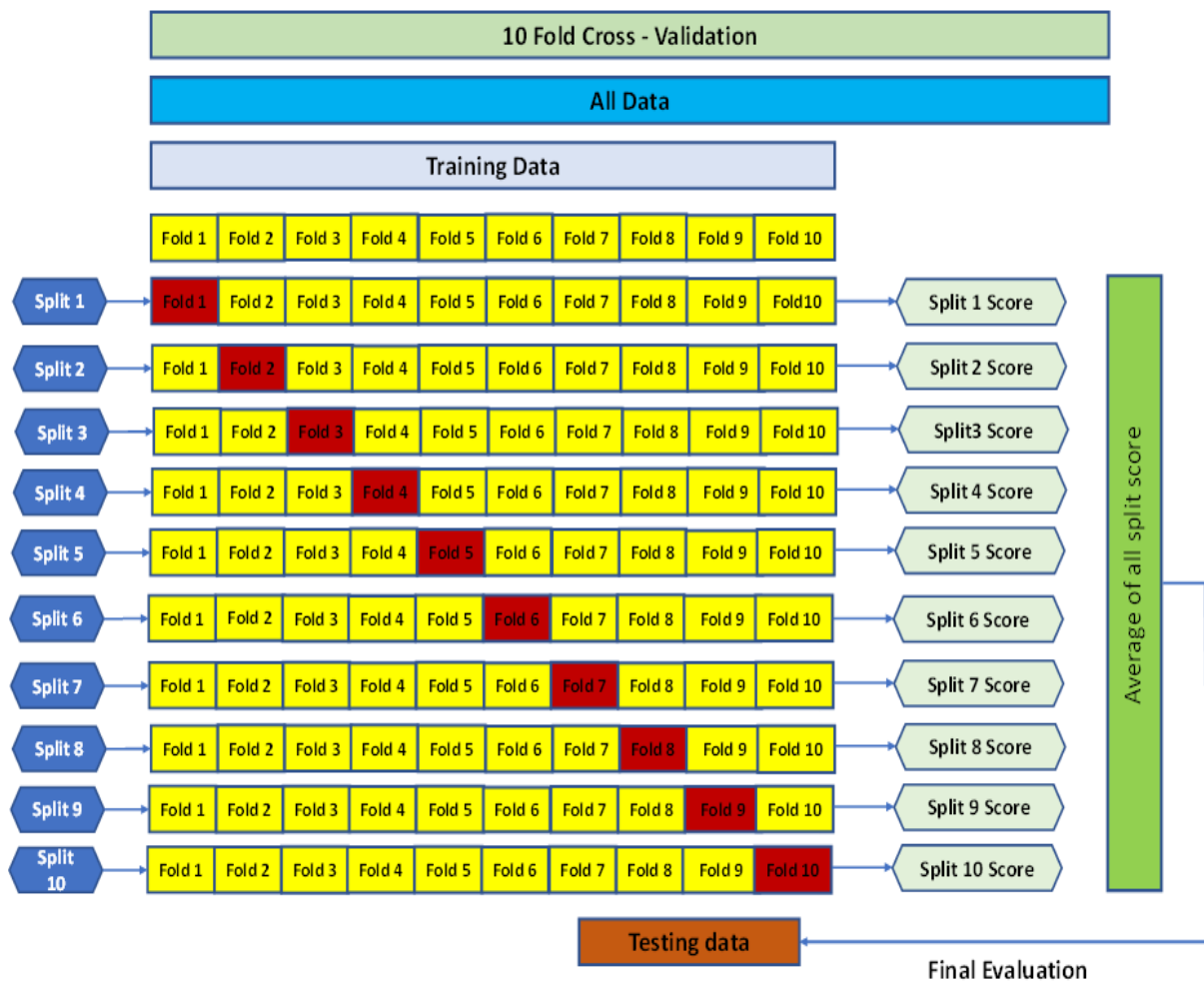


**Fig. 2.** Illustration of 10-Fold Cross-Validation

During the application of each input  $x_k$  to the network, the network's output is compared to the target. The difference between the goal and network outputs is used to compute the error. The objective is to keep the average of these mistakes as low as possible. In succeeding iterations, the neural network alters the weights between layers until the network can create the system's intended output within a defined accuracy or until the completed user-provided number of iterations. The weights on the connections between the neurons efficiently learn and store knowledge. It is expected that after training, the neural network would be able to create the appropriate output, such as problems that were not addressed during training. The backpropagation algorithm is the most extensively used continuous function mapping training approach. It has been demonstrated to be theoretically sound [35], performs well when modeling nonlinear processes, and is easy to write. The input to output mapping is developed using a backpropagation technique that minimizes a sum squared error cost function across a collection of training instances.

### 3.2. K-Fold cross-validation

Holding aside a portion of the data as a validation set is expected in supervised machine learning problems. K-Fold cross-validation [36] is utilized in this research to avoid overfitting and fully use the data used to train the model. The validation set is no longer required when using this approach. The data set is divided into ten folds here. The first fold is used to test the model, while the remaining folds train the model in the first iteration. This procedure is continued until each of the ten folds has served as a testing set. The overall structure of the 10-Fold cross-validation employed in this study is shown in Fig. 2.

### 3.3. Performance assessment

We used four statistical measures to evaluate the performance of the artificial neural network model in this article, namely the coefficient of determination ( $R^2$ ), root mean squared error (RMSE), mean absolute error (MAE), and mean absolute percentage error (MAPE). As seen, the

coefficient  $R^2$  indicates that there is a positive relationship between the actual value and the predicted value. The RMSE is used to evaluate the difference between the actual and predicted values, while the MAE displays the average error between the actual and predicted values, and the MAPE is defined as the difference between the actual value and the predicted value when the predicted value is compared to the actual value. The correctness of a model is determined by the values of RMSE, MAE, and MAPE. In contrast, a higher  $R^2$  score implies that the model is doing better. There are many possible values for  $R^2$  in the range of 0 and 1. The closer the value of  $R^2$  is to 1, the more accurate the model is. Definitions of four statistical indicators are given as follows:

$$R^2 = 1 - \frac{\sum_{i=1}^n (P_i - \hat{P}_i)^2}{\sum_{i=1}^n (P_i - \bar{P})^2} \quad (2)$$

$$RMSE = \sqrt{\frac{1}{n} \sum_{i=1}^n (P_i - \hat{P}_i)^2} \quad (3)$$

$$MAE = \frac{1}{n} \sum_{i=1}^n |P_i - \hat{P}_i| \quad (4)$$

$$MAPE = \frac{1}{n} \sum_{i=1}^n \left| \frac{P_i - \hat{P}_i}{P_i} \right| \quad (5)$$

where  $\hat{P}_i$  and the  $P_i$  is the target and the prediction of the  $i$ -th sample, respectively;  $\bar{P}$  is the average of the predicted outputs,  $n$  is the number of samples in the database.

## 4. Results and Discussion

### 4.1. Typical prediction results

As ANN training progresses, it becomes more important to understand how hidden layers, the number of neurons in each layer, and activation functions affect the model performance. Among the other concerns are the network's number of input and output variables, data quantity and noise, and network training approaches. Trial and error test is often used to determine the number of hidden layers and neurons in each layer. Experiments are performed to establish the exemplary network architecture. The ANN model with one hidden layer, however, has been demonstrated to properly

replicate the complicated interplay between input and output variables, even though it only comprises only one hidden layer [37]. It has been suggested by Nagendra [38] that the number of neurons in a hidden layer is dictated by the total number of neurons in the input and output layers combined. For the purpose of this investigation, a single hidden layer and thirteen neurons were employed in the ANN architecture. The linear activation function of the hidden layer is sigmoid, and the sigmoid linear activation function of the output layer is also a sigmoid function. With respect to the ANN model with the structure [12-13-1] selected, in the next section, the model's performance is evaluated in detail using statistical criteria such as  $R^2$ , RMSE, MAE, and MAPE and performed 10-fold CV.

In this phase, when the ANN model achieves optimal predictive performance on the training dataset, it will be evaluated on the test dataset. The training dataset (accounting for 70% of the samples) was divided into 10 parts to conduct cross-validation. With 10 such simulations, the forecast evaluation criteria will be averaged. Finally, the testing dataset (which accounts for the remaining 30% of data) is used to test the model's predictive ability for unknown data. The results of the ANN model prediction performance evaluation for both data sets are shown in Fig. 3, with 10 different simulations.

It can be seen that the predictive power of the ANN model changes when the training dataset changes. For the training data set, the performance evaluation criteria all vary within certain intervals, but the amplitude of oscillation is judged to be relatively stable:  $R^2$  fluctuates around 0.993, with the best run having the value  $R^2 = 0.995$  and the worst run is  $R^2 = 0.99$ , corresponding to CV8 and CV9, respectively. Herein, it is denoted the 8<sup>th</sup> and 9<sup>th</sup> simulation as CV8 and CV9, respectively. Similar statement is verified by RMSE error, when it ranges from 6.570 to 8.555, and the best, worst simulations are CV8 and CV9, respectively. The MAE assessment criteria have a value in the range

of 4.613 to 6.015 and are best at CV4, and worst at CV5. The MAPE criterion's minimum value is 4.818, and the maximum value is 6.895 for CV8 and CV5, respectively. Thus, the trained ANN model has excellent predictive power with the training data set selected for testing on the testing dataset.

Consider a testing dataset consisting of 48 experimental samples that are completely unknown during the training phase. It can be noticed that the proposed ANN model after 10-fold CV has perfect predictive power. Furthermore, there is no overfitting phenomenon because the capacity of ANN on the training set is better than the testing data set. The ANN model when forecasting new data gives quite good results, with the mean values of  $R^2$ , RMSE, MAE and MAPE in the range [0.972; 0.989], [13,389; 28.205], [9.555; 15,955] and [8.973; 13,785]. All four criteria give CV7 the best simulation. It can be seen that the difference here is negligible, and overall, the ANN model still gives an excellent predictive performance  $R^2 = 0.989$ . With such high accuracy, engineers can use this model to quickly predict the shear resistance of CRC beams.

In this next part, the typical predictive results of CV7 are selected for presentation, and this result is selected according to the criteria in considering the model's predictive ability for the test data set. It is demonstrated in Fig. 4 that the shear resistance values obtained from the tests, as well as those predicted by an artificial neural network (ANN) model. According to the ANN model, the prediction results for each sample and simulation are practically in good agreement, which suggests that the ANN model's predictive power is remarkable.

Figs. 5a and 5b illustrate the probability distributions of errors in the training and testing datasets accordingly. Typically, the errors follow a normal distribution, with the highest probability around zero values. An assessment of errors demonstrates that the ANN model generates good results within a reasonable range for the training dataset. There is a substantial concentration of

errors at zero (Fig. 5a). Similarly, according to the statistical analysis, the ANN model predicted the best outcomes in the testing phase (Fig. 5b).

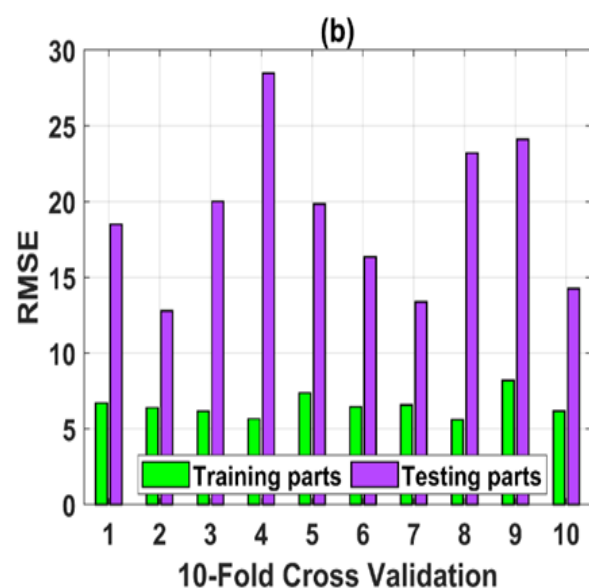
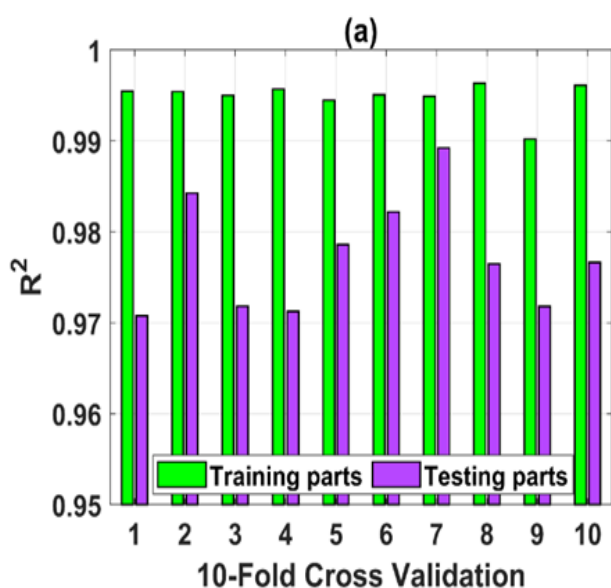
Fig. 6 presents the regression analysis for the training dataset (Fig. 6a) and the testing dataset (Fig. 6b). A diagonal line is drawn with a black dashed line in each figure, representing an excellent correlation for the problem ( $R^2 = 1$ ). In addition, the regression line is also shown by the pink line and often deviates slightly from the ideal regression diagonal. For each case, the predictors are calculated and shown:  $RMSE=6,570$ ,  $MAE=4.613$ ,  $R^2=0.995$ , and  $MAPE=4.818$  for the training dataset, and  $RMSE=13.389$ ,  $MAE=9.555$ ,  $R^2 = 0.989$  and  $MAPE = 8.973$  for the testing dataset.

**4.2. Comparison with Empirical Equations**

Additionally, five existing empirical models for the shear strength of CRC beams are compared with the proposed ANN model-based prediction model in this part to further assess and underline its superiority, including Xu and Niu's model [11], Huo's model [39], Li et al.'s model [40], Xue et al.'s model [33], and Lu et al.'s model [13].

The shear strength of the 158 CRC beams in the database is predicted using all five empirical models. In addition, the four indices,  $R^2$ , RMSE, MAE, and MAPE, also assess the models'

performance. Fig. 7 and Table 2 show the ANN model's prediction results and accuracy along with empirical formulas, respectively. It is easily seen that compared with the five models, the ANN model performs the best. Even when compared to the best empirical model, Xu and Niu's model, which has  $R^2 = 0.891$ ,  $RMSE = 37.529$  kN,  $MAE = 28.713$  kN, and  $MAPE = 26.512$ , the ANN model had  $R^2$ , RMSE, MAE, and MAPE improvements of 11.2%, 75.3%, 78.8%, and 77.16%, respectively. Among the other empirical models, Huo's model performs those proposed by Li et al. and Lu et al., while Xue et al.'s model has the lowest predictive capability. The major goal of this section was to show that the ANN technique, thanks to many advantages stated earlier, has a stronger prediction capability than the empirical model. The developed machine learning model is neither constrained nor restricted in terms of CRC beams type (depending on the ratio of shear span-to-depth). However, in the empirical equations, the criterion of beam type is considered when applying the formula. In addition, the empirical equations use coefficients related to the characteristics of the CRC beams. Therefore, these equations may be too secure, thus increasing the cost of structures. Once again, this highlights the benefits of the proposed unified ANN model in improving the prediction accuracy and generalizability.



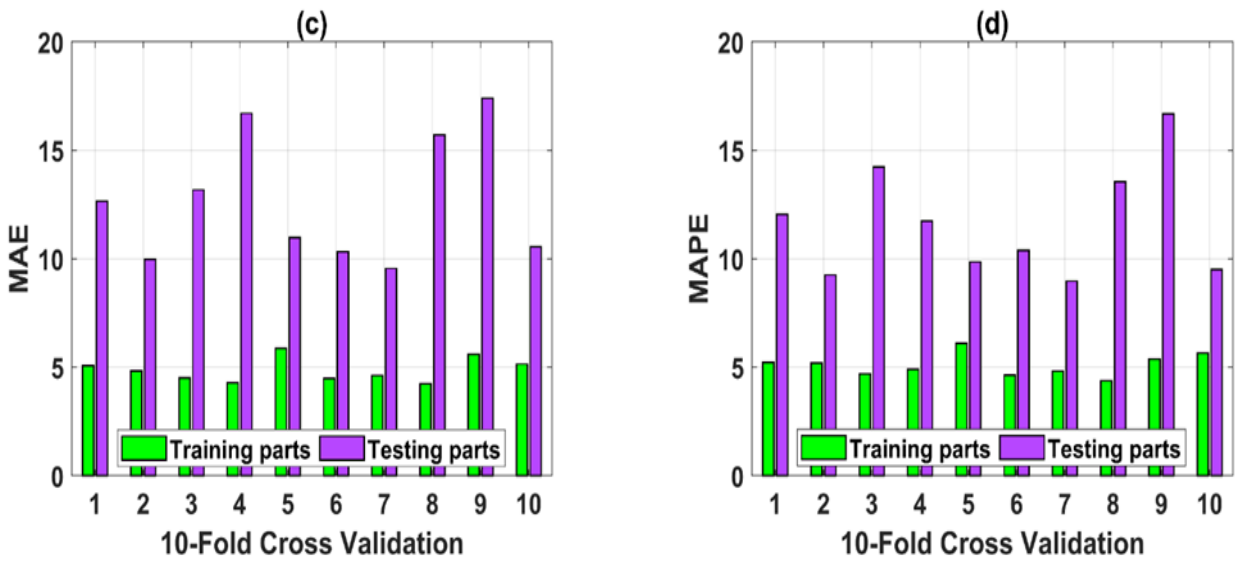


**Fig. 3.** Results of training of ANN model after 10-fold cross-validation based on different performance evaluation criteria: (a)  $R^2$ , (b) RMSE, (c) MAE, and (d) MAPE

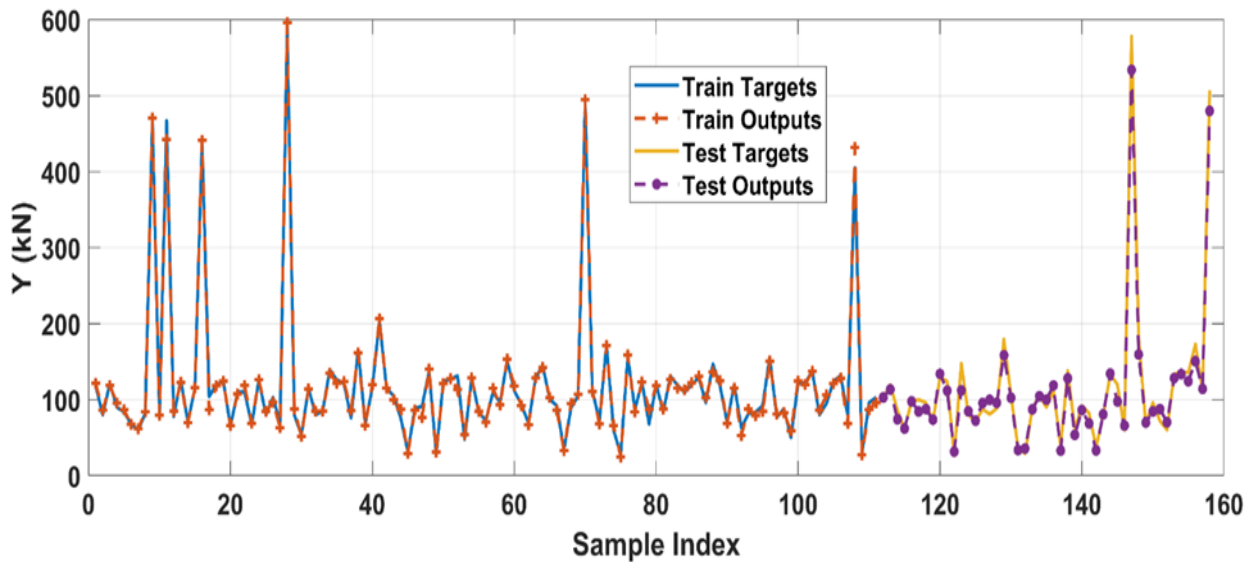


**Fig. 4.** Comparison of the performance of the ANN model with the actual values of the shear strength of CRC in the function of training dataset and testing dataset

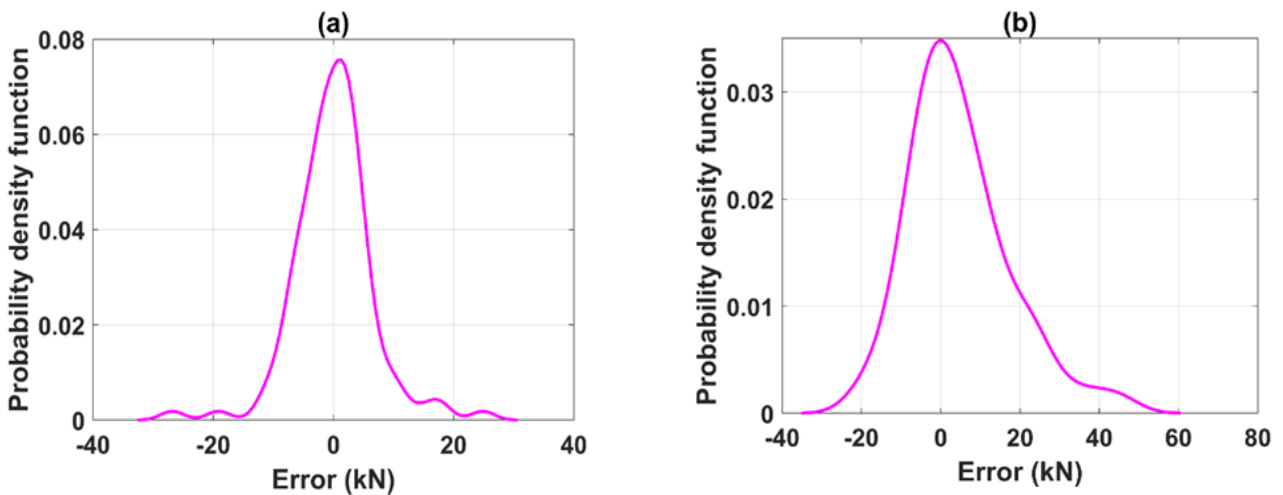


**Fig. 5.** Probability density of errors for (a) training dataset, and (b) testing dataset



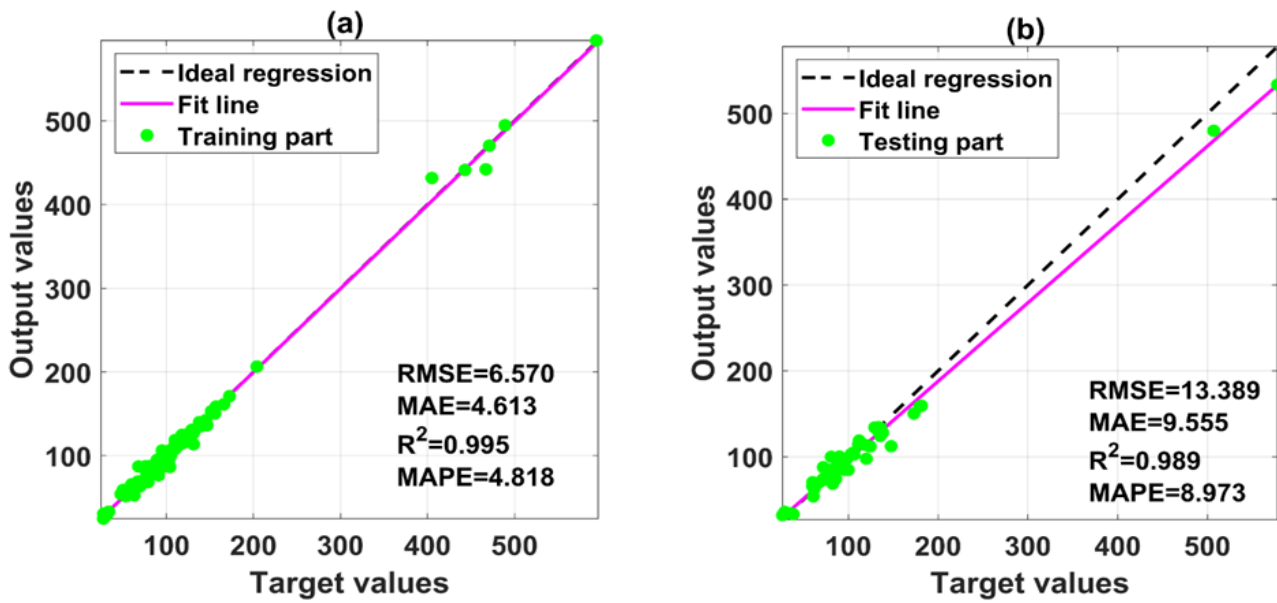
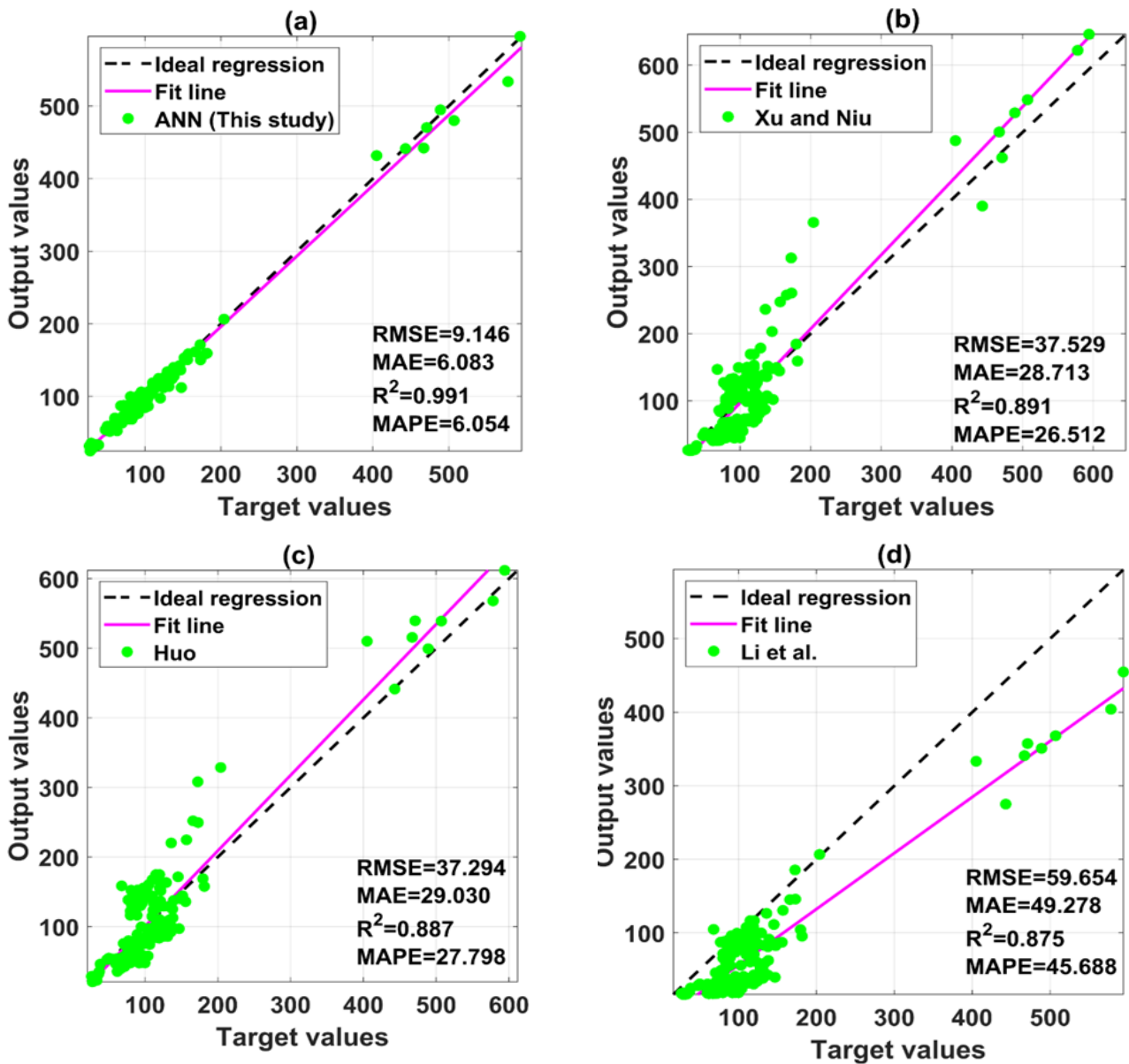
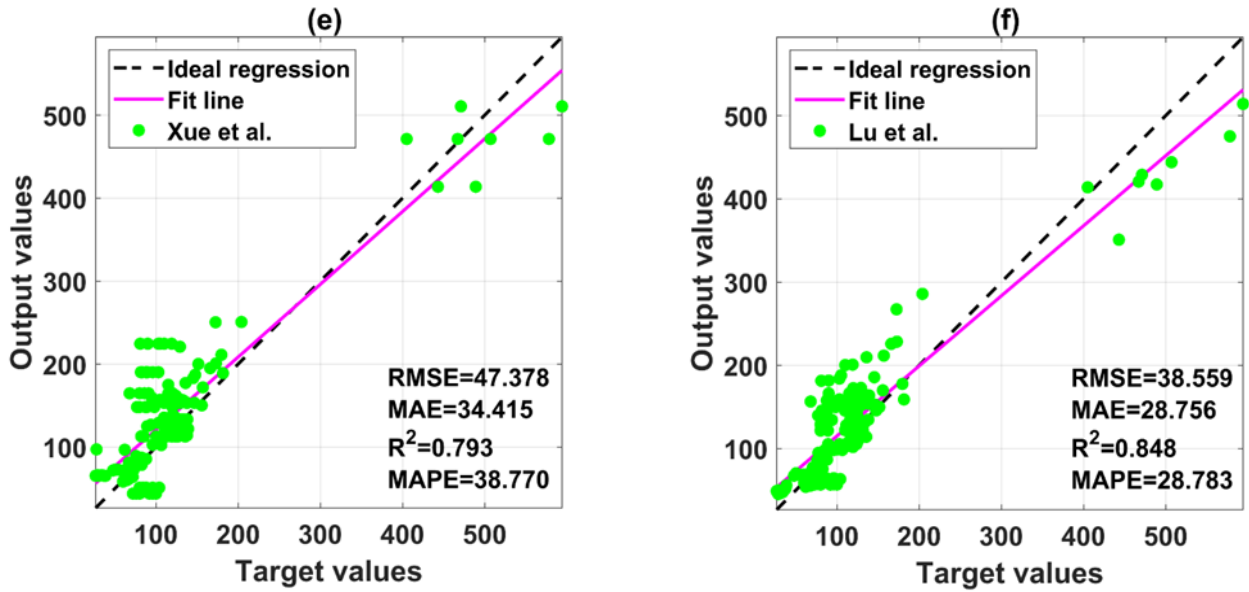


Fig. 6. Correlation between training part (a) and testing part (b)





**Fig. 7.** Comparison of methods for predicting the shear strength of CRC beams

**Table 2.** Performance measures for the empirical models and ANN model

Models	Performance measures			
	R <sup>2</sup>	RMSE (kN)	MAE (kN)	MAPE
Xu and Niu [11]	0.891	37.529	28.713	26.512
Huo [39]	0.887	37.294	29.030	27.798
Li et al. [40]	0.875	59.654	49.278	45.688
Xu et al. [33]	0.793	47.378	34.415	38.770
Lu et al. [13]	0.848	38.559	28.756	28.783
The proposed ANN	0.991	9.146	6.083	6.054

### 5. Conclusion

CRC beam shear strength was shown to be easily predicted using an ANN model in this study, which is a cost-effective method for reducing the amount of time and effort required for ongoing laboratory experiments, as well as increasing the accuracy of predictive models based on data gathered over time from previous studies. In order to train and assess the ANN model, 158 sets of CRC beam shear tests are gathered in the literature. The results of the 10-fold cross-validation method show that the ANN model has a high degree of accuracy in predicting the outcomes of experiments. The R<sup>2</sup> coefficient of determination was 0.989, suggesting that the model performed exceptionally well. Five empirical models for

predicting the shear strength of CRC beams were also used to assess the performance of the constructed ANN model. It is shown that the ANN model has the best prediction performance. This overcomes a limitation of traditional empirical or analytical models, which typically have few parameters. However, the current research is limited to forecasting the shear strength prediction performance of the ANN model and comparing it with experimental formulas. Variable reduction strategies in future work to increase the speed and efficiency of prediction should be considered. Simultaneously, sensitivity analysis should also be conducted to investigate the influence of input parameters on the target variable.

### Reference

- [1] C. Andrade, C. Alonso, F.J. Molina. (1993). Cover cracking as a function of bar corrosion: Part I-Experimental test. *Materials and structures*, 26(8), 453-464.
- [2] J.G. Cabrera. (1996). Deterioration of concrete due to reinforcement steel corrosion. *Cement and Concrete Composites*, 18(1), 47-59.
- [3] P.S. Mangat and M.S. Elgarf. (1999). Flexural strength of concrete beams with corroding reinforcement. *Structural Journal*, 96(1), 149-158.
- [4] G.J. Al-Sulaimani, M. Kaleemullah, and I.A. Basunbul. (1990). Influence of corrosion and cracking on bond behavior and strength of reinforced concrete members. *Structural Journal*, 87(2), 220-231.
- [5] A.V. Saetta and R.V. Vitaliani. (2004). Experimental investigation and numerical modeling of carbonation process in reinforced concrete structures: Part I: Theoretical formulation. *Cement and Concrete Research*, 34(4), 571-579.
- [6] C. Alonso, C. Andrade, J. Rodriguez, and J.M. Diez. (1998). Factors controlling cracking of concrete affected by reinforcement corrosion. *Materials and Structures*, 31(7), 435-441.
- [7] B. Fu and D.-C. Feng. (2021). A machine learning-based time-dependent shear strength model for corroded reinforced concrete beams. *Journal of Building Engineering*, 36, 102118.
- [8] I. Khan, R. François, and A. Castel. (2014). Experimental and analytical study of corroded shear-critical reinforced concrete beams. *Materials and Structures*, 47(9), 1467-1481.
- [9] C. Higgins, W.C. Farrow III, and O.T. Turan. (2012). Analysis of reinforced concrete beams with corrosion damaged stirrups for shear capacity. *Structure and Infrastructure Engineering*, 8(11), 1080-1092.
- [10] Y. Zhao and W. Jin. (2008). Analysis on shearing capacity of concrete beams with corroded stirrups. *Journal-Zhejiang University Engineering Science*, 42(1), 19.
- [11] X.U. Shanhu and N.I.U. Ditao. (2004). The shear behavior of corroded simply supported reinforced concrete beam. *Journal of Building Structures*, 5.
- [12] A.K. El-Sayed. (2017). Shear capacity assessment of reinforced concrete beams with corroded stirrups. *Construction and Building Materials*, 134, 176-184.
- [13] Z.-H. Lu, H. Li, W. Li, Y.-G. Zhao, and W. Dong. (2018). An empirical model for the shear strength of corroded reinforced concrete beam. *Construction and Building Materials*, 188, 1234-1248.
- [14] X. Xue and H. Seki. (2010). Influence of longitudinal bar corrosion on shear behavior of RC beams. *Journal of Advanced Concrete Technology*, 8(2), 145-156.
- [15] A.K. Azad, S. Ahmad, and B.H.A. Al-Gohi. (2010). Flexural strength of corroded reinforced concrete beams. *Magazine of Concrete Research*, 62(6), 405-414.
- [16] A.K. Azad, S. Ahmad, and S.A. Azher. (2007). Residual strength of corrosion-damaged reinforced concrete beams. *ACI Materials Journal*, 104(1), 40.
- [17] A. Ouglova, Y. Berthaud, F. Focht, M. François, F. Ragueneau, and I. Petre-Lazar. (2008). The influence of corrosion on bond properties between concrete and reinforcement in concrete structures. *Materials and Structures*, 41(5), 969-980.
- [18] Q.H. Nguyen *et al.* (2020). A novel hybrid model based on a feedforward neural network and one step secant algorithm for prediction of load-bearing capacity of rectangular concrete-filled steel tube columns. *Molecules*, 25(15), 3486.
- [19] T.-A. Nguyen, H.-B. Ly, and V.Q. Tran. (2021). Investigation of ANN Architecture for Predicting Load-Carrying Capacity of Castellated Steel Beams. *Complexity*, 2021.
- [20] H.-B. Ly, M.H. Nguyen, and B.T. Pham. (2021). Metaheuristic optimization of Levenberg–Marquardt-based artificial neural network using particle swarm optimization for prediction of foamed concrete compressive strength. *Neural Computing and Applications*, 33(24), 17331-17351.
- [21] P.G. Asteris, L. Cavaleri, H.-B. Ly, B.T. Pham.

- (2021). Surrogate models for the compressive strength mapping of cement mortar materials. *Soft Computing*, 25(8), 6347-6372.
- [22] H.-V.T. Mai, T.-A. Nguyen, H.-B. Ly, and V.Q. Tran. (2021). Investigation of ANN Model Containing One Hidden Layer for Predicting Compressive Strength of Concrete with Blast-Furnace Slag and Fly Ash. *Advances in Materials Science and Engineering*, 2021.
- [23] B.T. Pham *et al.* (2020). Development of artificial neural networks for prediction of compression coefficient of soft soil. *CIGOS 2019, Innovation for Sustainable Infrastructure*, Springer, 2020, pp 1167–1172.
- [24] Q.H. Nguyen *et al.* (2021). Influence of data splitting on performance of machine learning models in prediction of shear strength of soil. *Mathematical Problems in Engineering*, 2021.
- [25] T.-A. Nguyen, H.-B. Ly, H.-V.T. Mai, and V.Q. Tran. (2021). Using ANN to Estimate the Critical Buckling Load of Y Shaped Cross-Section Steel Columns. *Scientific Programming*, 2021.
- [26] Q.H. Nguyen, H.-B. Ly, T.-A. Nguyen, V.-H. Phan, L.K. Nguyen, and V.Q. Tran. (2021). Investigation of ANN architecture for predicting shear strength of fiber reinforcement bars concrete beams. *Plos one*, 16(4), e0247391.
- [27] H.-B. Ly, T.-T. Le, H.-L.T. Vu, V.Q. Tran, L.M. Le, and B.T. Pham. (2020). Computational hybrid machine learning based prediction of shear capacity for steel fiber reinforced concrete beams. *Sustainability*, 12(7), 2709.
- [28] J. Rodriguez, L.M. Ortega, and J. Casal. (1997). Load carrying capacity of concrete structures with corroded reinforcement. *Construction and Building Materials*, 11(4), 239-248.
- [29] C. Higgins and W.C. Farrow III. (2006). Tests of reinforced concrete beams with corrosion-damaged stirrups. *ACI Materials Journal*, 103(1), 133.
- [30] X. LI and H. YIN. (2010). Degradation Mechanism and Predicting Models of Shearing Capacity for Corroded Reinforced Concrete Beams. *Journal of Xuzhou Institute of Technology (Natural Sciences Edition)*, 4.
- [31] J. Xia, W. Jin, and L. Li. (2011). Shear performance of reinforced concrete beams with corroded stirrups in chloride environment. *Corrosion Science*, 53(5), 1794-1805.
- [32] C.A. Juarez, B. Guevara, G. Fajardo, P. Castro-Borges. (2011). Ultimate and nominal shear strength in reinforced concrete beams deteriorated by corrosion. *Engineering Structures*, 33(12), 3189-3196.
- [33] X. Xue, H. Seki, and Z. W. Chen. (2013). Shear capacity of rc beams containing corroded longitudinal bars. *Proceedings of the Thirteenth East Asia-Pacific Conference on Structural Engineering and Construction (EASEC-13)*, 2013, p. C–6.
- [34] S. Liu. (2013). The research on shear capacity of corroded rc beams. PhD Thesis, Master's thesis, Central South University, China.
- [35] D.E. Rumelhart, G.E. Hinton, R.J. Williams. (1985). Learning internal representations by error propagation. California Univ San Diego La Jolla Inst for Cognitive Science.
- [36] R. Kohavi. (1995). A study of cross-validation and bootstrap for accuracy estimation and model selection. *Ijcai*, 14(2), 1137-1145.
- [37] G. Cybenko. (1989). Approximation by superpositions of a sigmoidal function. *Mathematics of Control, Signals and Systems*, 2(4), 303-314.
- [38] S. Nagendra. (1998). Practical Aspects of Using Neural Networks: Necessary Preliminary Specifications. *Technical Paper, GE Research and Development Center*.
- [39] H. Yanhua. (2006). Research on shear capacity of simply supported concrete beam with corroded reinforcement. *Industrial Construction*, 36(S1), 910-912.
- [40] L.I. Shi-bin and Z. Xin. (2011). Analysis for shear capacity of reinforced concrete beams with corrosion stirrups. *Engineering Mechanics*, 28(1), 60-63.